Novel Methodology for Investigating Electrochemical Gas Evolution Reactions: Floating Electrode as a Means for Effective Gas Bubble Removal

Primož Jovanovič*[§], Kevin Stojanovski[§], Marjan Bele[†], Goran Dražić[†], Gorazd Koderman Podboršek[†], Luka Suhadolnik[⊥], Miran Gaberšček[†,‖], Nejc Hodnik[§]

[§]Department of Catalysis and Chemical Reaction Engineering, National Institute of Chemistry, Hajdrihova 19, SI-1000 Ljubljana, Slovenia

[†]Department of Materials Chemistry, National Institute of Chemistry, Hajdrihova 19, SI-1000 Ljubljana, Slovenia

[⊥]Department for Nanostructured Materials, Jožef Stefan Institute, Jamova 39, SI-1000 Ljubljana, Slovenia

[‖]Faculty of Chemistry and Chemical Technology, University of Ljubljana, Večna pot 113, SI-1000 Ljubljana, Slovenia

Corresponding author: primoz.jovanovic@ki.si

Supporting Information

The present supporting materials include additional characterization data based on TEM, SEM and electrochemical analysis.

Table of Contents

S-1 Details of the floating electrode system

Details of the metallic spring: The spring used in the floating electrode setup is commercially used in chemical pens (PILOT CORPORATION OF EUROPE, PAE de La Caille – Saint-Martin BELLEVUE – 74 350 Allonzier –La – Caille, France, Product Code: Pilot G2 Gel Pen - 0.7 mm), Length; 19 mm, diameter; 5 mm.

Details of the metallic cone: Inner diameter 3 mm (see Scheme S-2).

Details of the vacuum suction tube: Outer diameter 3 mm, inner diameter 1 mm.

Details of the Cu foil: The following Cu foil was used; thickness

The entire three electrode electrochemical cell used in the floating electrode configuration is shown in Scheme S-1.

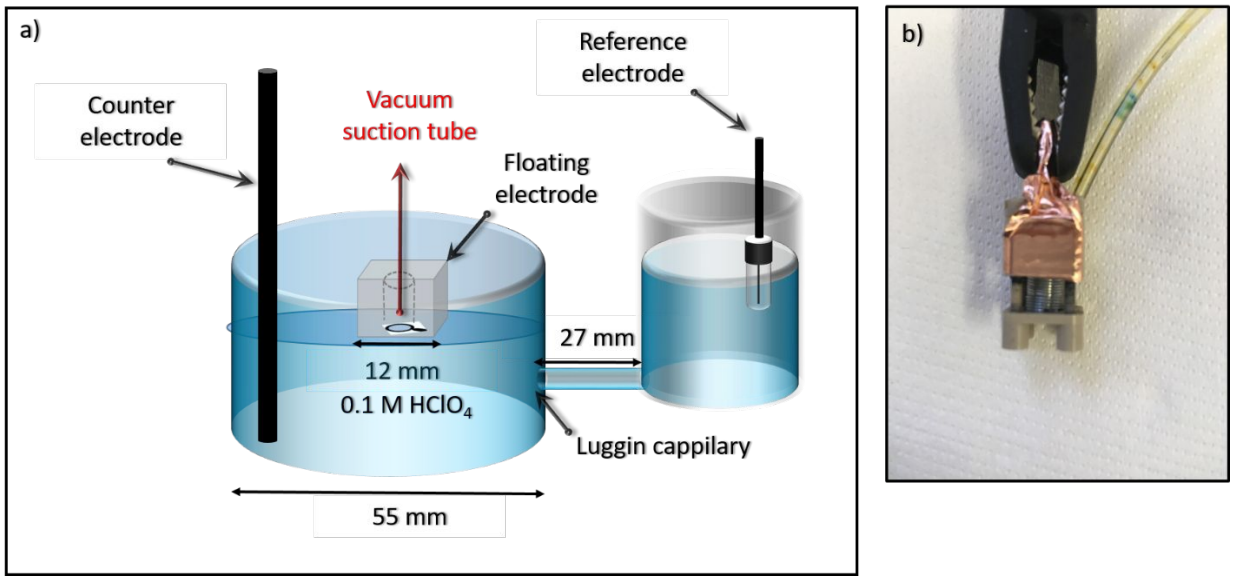

Scheme S-1: a) Schematic presentation of the electrochemical cell configuration. b) Real image of the floating electrode configuration demonstrating electric contacts, Cu foil and vacuum suction tube.

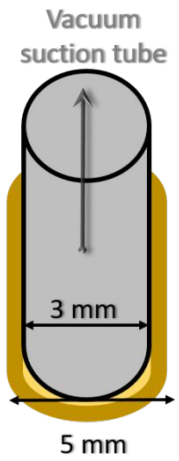

Scheme S-2: Schematic presentations of the metallic cone used in the floating electrode setup.

S-2 Vacuum suction methodology

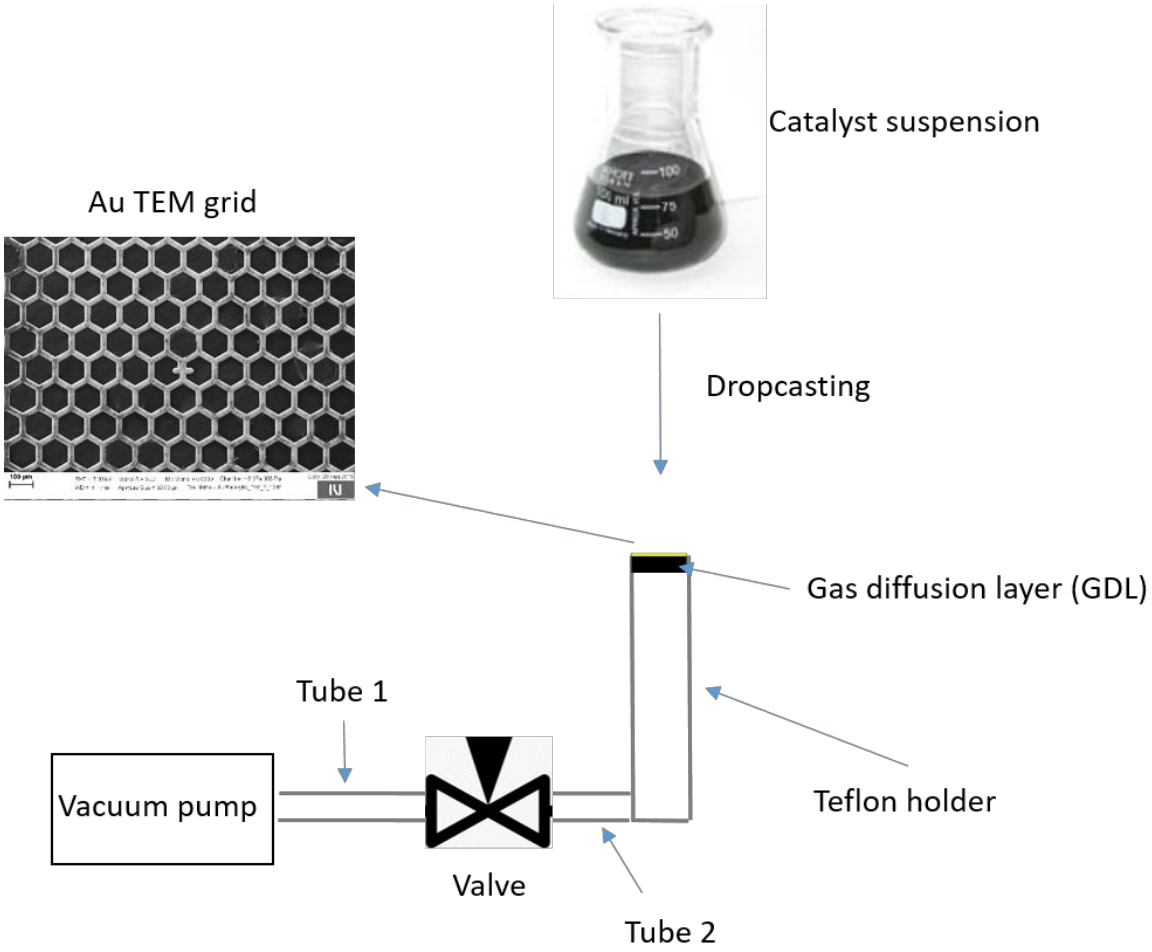

Figure S-1: Schematic diagram of the vacuum suction methodology used to prepare the catalyst layer. Rubber tube 1 and 2 have the same inner diameter (5 mm).

A vacuum pump from producer Ted Pela was used in film preparation as well as during electrochemical experiments. An easy-affordable vacuum pump (Ted Pella, PELCO® 520-220) that was used to induce vacuum suction is conventionally used to manipulate with TEM grids. Hence its vacuum suction strength cannot be determined. The pump and valve characteristics are given bellow:

- The vacuum system is powered by a 220V, (50 Hz) cycle low wattage vibrator-type pump. The in-line filter is placed adjacent to the pump with the four foot plastic hose following.
- Vacuum suction level: In order to regulate vacuum suction a special micrometer valve (Stainless Steel Integral Bonnet Needle Valve, 0.37 Cv, 1/4 in. Swagelok Tube Fitting, Regulating Stem, **Part No.** SS-1RS4) was used to manipulate with vacuum strength during **i)** electrochemical experiment and **ii)** during deposition of the catalyst suspension. However, we note that manipulation with a vacuum can only be performed in a relative manner. This means that if the valve is entirely opened the level is labelled as 1. If the valve is opened only till half the level is labeled as 0.5 etc.

- Tubings: In the case of vacuum suction used to prepare the catalyst layer the following tubing configuration was used (see Fig. S-1).
- Film drying conditions: After dropcasting the drop of catalyst was dried for 30 min under vacuum suctions conditions (vacuum level 1)

S-3 Scanning electron microscopy characterization

Catalyst deposits on TEM grids were investigated using a scanning electron microscope (FE-SEM Zeiss SUPRA 35VP) with an accelerating voltage of 7 kV**.**

Catalyst films on the TEM grid were prepared either by dropcasting an aqueous suspension of the catalyst on the TEM grid followed by drying under **i)** ambient conditions (Fig.S1 a,b) or by dropcasting the aqueous suspension of the catalyst on the TEM grid and **ii)** subsequent drying by using a vacuum suction (Fig.S1 c,d). The vacuum suction causes fast evaporation of water from the catalyst suspension. Comparison of the two preparation modes **i)** and **ii)** reveals the beneficiary effect of the vacuum preparation method as the catalyst film coverage is more uniform in the latter case.

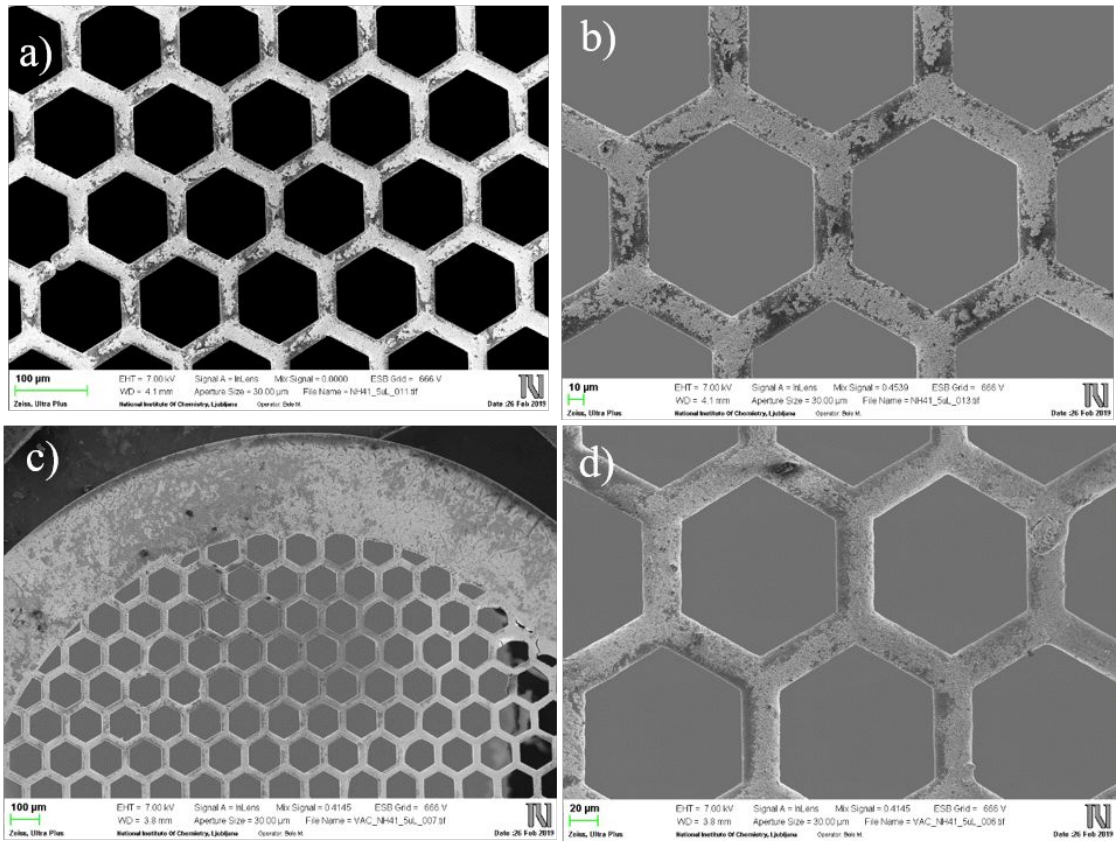

Figure S-2: SEM image of the Au TEM grid used in electrochemical experiments. In the case of a) and b) the catalyst was deposited by dropcasting the suspension which was afterwards dried under ambiental conditions. In the case of c) and d) the suspension of the catalyst was dried using a vacuum suction.

S-4 Synthesis of high surface area iridium-based nanoparticles

For the proof of concept, an in-house synthesized high surface area nanoparticulate iridium was used as a model OER electrocatalyst (see Fig. S2). It was prepared by dissolving 100 mg of iridium(III) bromide hydrate (CAS number: 317828-27-6, Sigma-Aldrich, St. Louis, MO) in 3 mL of ultra pure water (18.2 $m\Omega cm^{-1}$, Milli-Q®) at 50 °C. The solution was then mixed with 0.5 g of hydrazine hydrate (50-60 %, CAS number: 10217-52-4, Sigma-Aldrich, St. Louis, MO) at 50 °C until water evaporation. Afterwards, the dry residue was thermally treated in a 5% H_2/Ar mixture. The temperature was increased to 450 °C with a rate of 2 °C min^{-1}, and then cooled to room temperature with a rate of 3 °C min^{-1}.

X-ray powder diffraction pattern for the analysis was collected at room temperature on a laboratory PANalytical X'Pert PRO diffractometer using CuKa radiation (1.54060 Å). Sample was loaded into a flat disc-like sample holder. The XRD data were collected in the 2θ range from 30 to 60° in steps of 0.04° 2θ with a total measurement time of 12.5 min. Phase identification was performed in the X'Pert HighScore Plus program using the International Centre for Diffraction Data (ICDD) PDF-4+ 2016 database [1]. In the diffractogram of sample two diffraction peaks appear which are related to cubic Iridium at 2θ = 40.8° (111) and 47.4° (200) angles (PDF 03-065-1686) [1].

Literature:

1. ICDD. PDF-4+ 2016 (Database); Kabekkodu, S., Ed.; International Centre for Diffraction Data: Newtown Square, PA, USA, 2016.

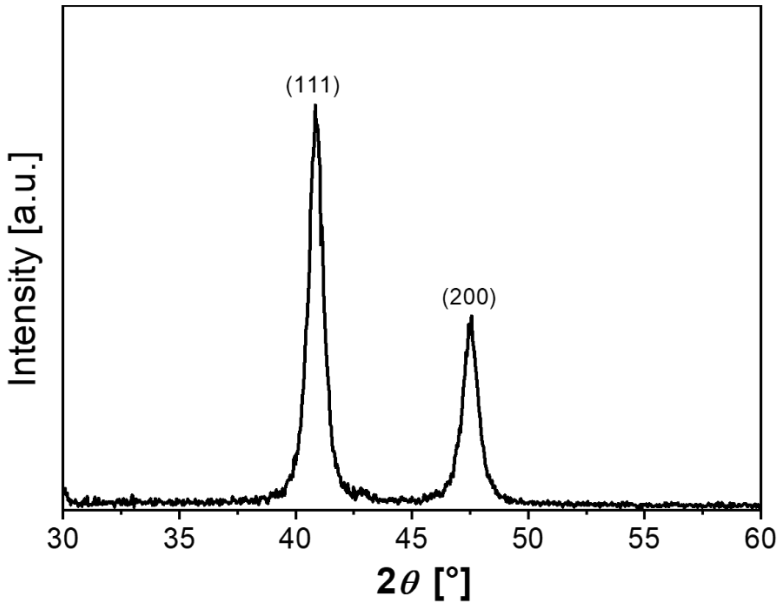

Figure S-3: XRD diffractogram of the synthesized Ir nanoparticles.

S-5 Transmission electron microscopy characterization

For the detailed microstructural investigation, Cs probe corrected Scanning transmission electron microscope (Jeol ARM 200 CF) with attached Jeol Centurio EDXS system with 100mm^2 SDD detector and Gatan Quantum ER DualEELS system was used**.**

Wire-like particle morphologies of iridium based electrocatalyst are observed in the TEM imaging. This reflects the agglomeration of primary particles during heat treatment.

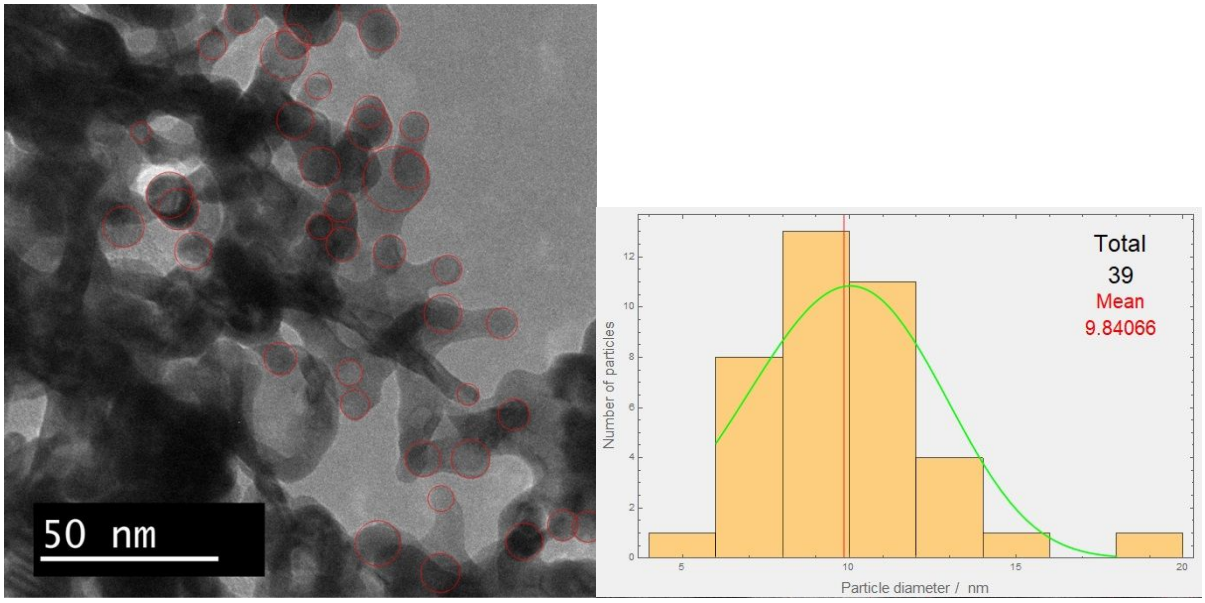

Figure S-4: Sampling and histogram for Ir electrocatalyst used in the study.

S-6 Feasibility of the Au TEM grid as the working electrode

Prior to electrochemical testing of electrocatalyst electrochemical performance of bare Au TEM grid was inspected. Characteristic features of Au were followed via cyclovoltammtery by gradually increasing the upper potential limit (UPL). From the results (Fig.S3) it is clearly seen that characteristic redox features are obtained.

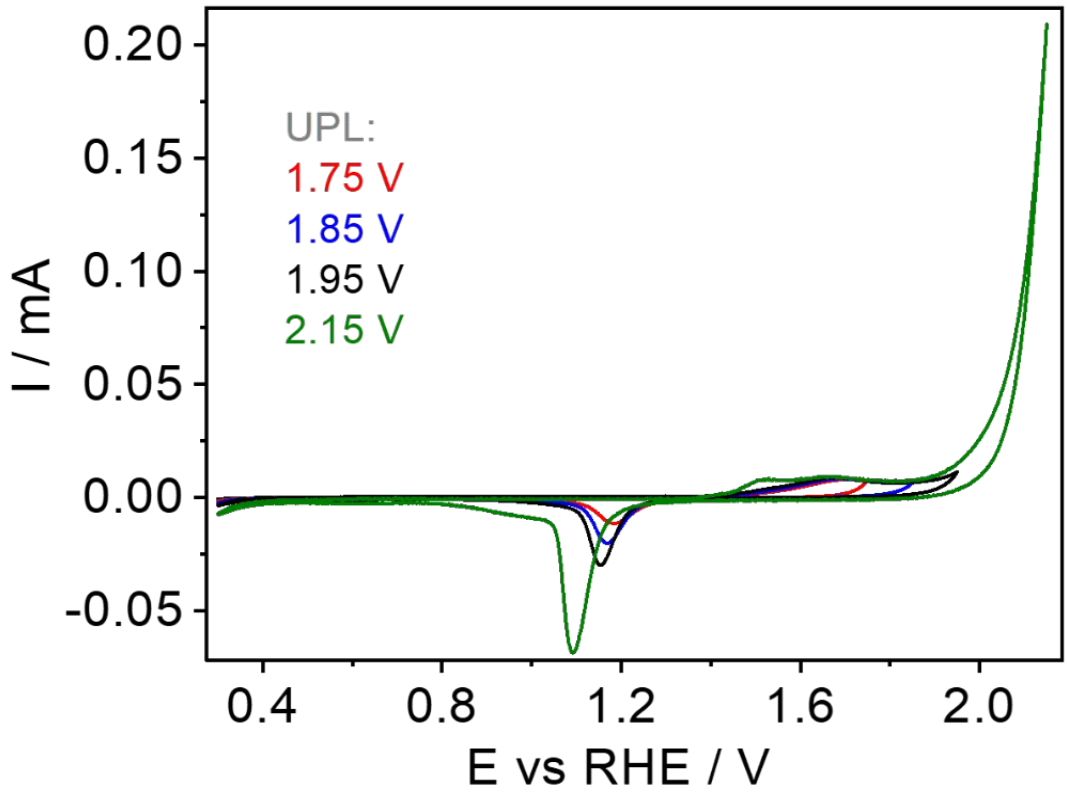

Figure S-5: Cyclovoltammetric response of bare Au grid in the floating electrode configuration by gradually increasing UPL. Each measurement started at 0.3 V vs RHE. Measurements were performed in 0.1 M $HClO_4$, scan rate 100 mVs^{-1}.

S-7 Feasibility of the floating electrode configuration:

a) Loading effect

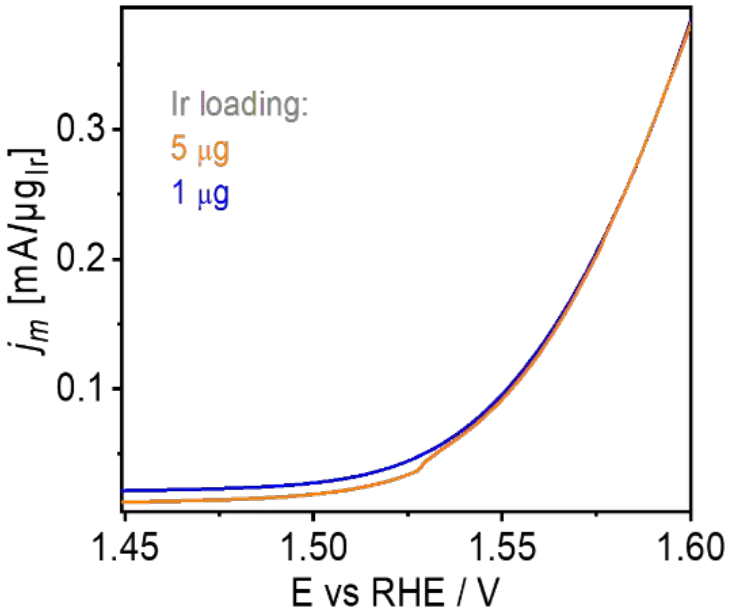

Figure S-6: Linear sweep LSV polarization curves in the case of two different loadings (20 mVs^{-1}).

b) Potentiostatic treatment of Au TEM grid coated with catalyst layer as floating electrode at 2.0 V vs RHE

The feasibility of the floating electrode to efficiently remove the oxygen bubbles was tested during a potentiostatic (2.0 V vs RHE) treatment. Two modes of operation were compared. In the first case vacuum suction was present during potentiostatic treatment (blue curve) and in the second case vacuum suction was absent (black curve). Even though potentials of this range are rather severe for simulating degradation of the catalyst in our study they are used in order to maximize the evolution of bubbles. Chronoamperometric response normalized per mass of iridium is shown in Fig. S6. The performance of the two electrode configuration (*vacuum* and *non-vacuum-ambiental*) were compared (Fig. S6). Chronoamperometric performance (mass current densities) in the case of the *vacuum* case is surpassing the *non-vacuum* case. This can be assigned to the use of vacuum. This has triggered the appearance of two effects: **i)** higher utilization of the catalyst layer hence a larger effective surface area in *vacuum* analogue in comparison to *non-vacuum* case. **ii)** Additionally, given the fact that substantially different shape of chronoamperometric response is detected for the *vacuum* analogue the higher current densities of the *vacuum* analogue electrode should also be ascribed to more efficient removal of oxygen bubbles which leads to more exposed surface area. It is noted here that in the case of *non-vacuum-ambiental* experiment a complete bubble passivation of the electrode occurred hence the experiment was stopped after approximately 800 s in this case. This is why only one dash curve is shown in Fig. S6d as one cannot refer to decaj in performance in a proper sense. More specific, if such TEM grid (which is passivated with bubbles) is de-passivated mechanically (for example by removing from the electrode

compartment) and the its LSV response is re-analyzed almost the same performance as prior potentiostatic treatment is obtained (data not shown).

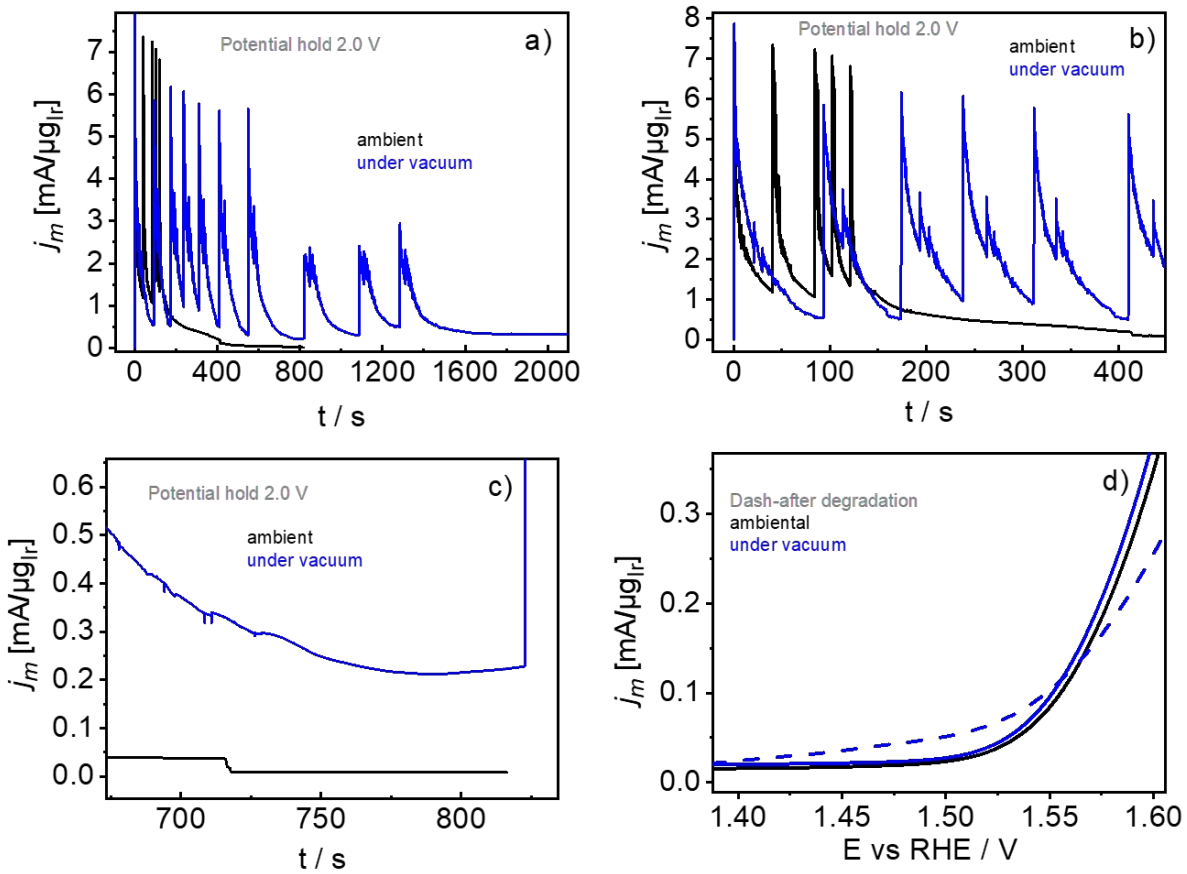

Figure S-7: A comparison of electrochemical response of the floating electrode in the case of ambient conditions (black curves) and when vacuum suction (relative vacuum level 1) was used (blue curve). a) Potential hold treatment at 2.0 V vs RHE. We note that potentiostatic treatment was stopped after approximately 800 s in the case of ambient analogue due to complete passivation of the electrode in the case of ambient analogue.b) Magnification of chronoamperometric curves. c) Magnification of chronoamperometric curves indicating the complete passivation of the electrode in the case of ambient analogue. d) LSV performance of the two analogues. We note that no LSV polarization curve was recorded in the case of ambient analogue because the electrode was completely passivated with oxygen bubbles.

c) Vacuum suction effect

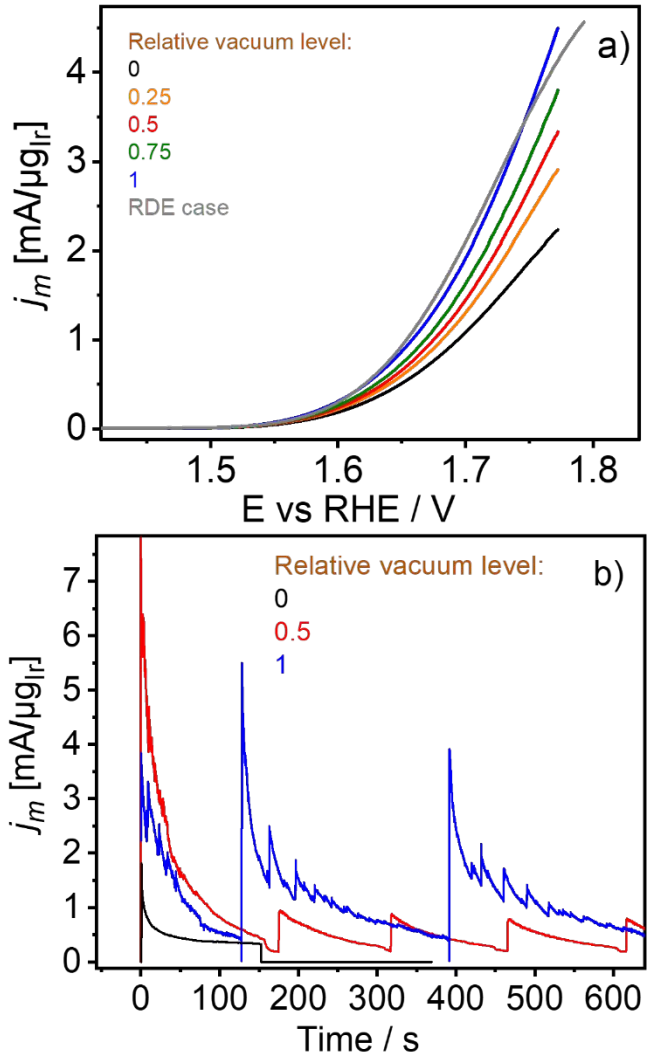

Figure S-8: Electrochemical response of the floating electrode in the presence of vacuum suction. a) Mass normalized linear sweep voltammetric polarization curves (LSV) under the conditions of different levels of vacuum suction during ongoing OER (scan rate 20 mVs^{-1}). For comparison, a LSV polarization curve obtained in RDE configuration (grey curve) is shown (20 mVs^{-1}, rotation 1600 RPM). b) Mass normalized chronoamperometric response under the conditions of different levels of vacuum suction under potential of 1.8 V vs RHE.

S-8 Performance of the floating electrode vs RDE configuration:

The electrochemical performances of the floating electrode (*vacuum* case analogue) and RDE configuration were compared. Potentiostatic treatment in the case of the floating electrode was performed at 2.0 V and at 1.8 V (both for 2000 s) in the case of RDE. Before and after potentiostatic treatment LSV protocol was performed in order to estimate OER activity (Fig.S5). Interestingly, retention of OER activity after potentiostatic treatment is lower in the case of RDE configuration despite being treated at a lower potential (1.8 V). This trend is in line with the fact that oxygen bubbles passivate the electrode surface in the RDE configuration. Hence the effective catalyst surface is lower in this case. However, it has to be noted that further optimization of the floating electrode architecture is necessary in order to maximize the removal of the oxygen bubbles.

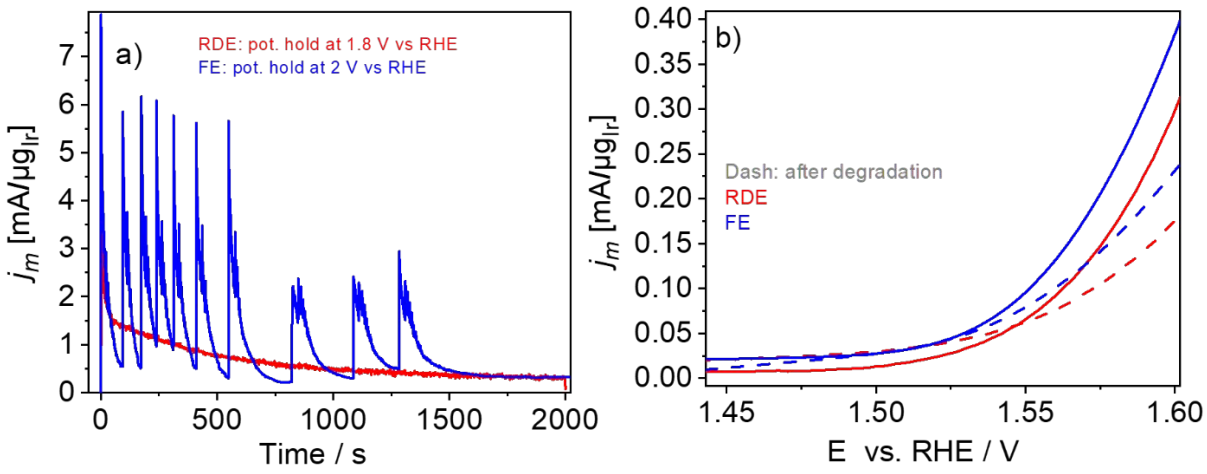

Figure S-9: Comparison of electrochemical performances of floating electrode and RDE configurations. a) Potentiostatic treatment. b) LSV treatment before (solid lines) and after potentiostatic (dash) treatment; scan rate 20 mVs^{-1}.

S-9 Indirect confirmation of oxygen bubble effect in RDE configuration:

In order to indirectly confirm that oxygen bubbles are being evolved in the course of OER potentiostatic treatment, the following experiment was performed in RDE configuration. The catalayts was treated under three modes of potentiostatic treatment: **i)** Initially potential of 1.8 V was used to perform OER after which **ii)** second potentiostatic treatment was performed under conditions of the oxygen reduction reaction (5 min at 0.3 V vs. RHE (Fig. S6). The subsequent potential hold is not shown. The purpose of **ii)** was to electrochemically reduce the oxygen bubbles formed during treatment **i)**. After treatment **ii)** potential was set to 1.8 V again (treatment **iii**) in order to compare the corresponding current response to the one of **i)**. Alltogether, treatment i) lasted 35 min. The chronoamperometric responses of **i)** and **iii)** are shown in Fig. S6. These results clearly indicate that oxygen bubbles are formed during potentiostatic treatment at 1.8 V (Fig. S6b-blue curve). More specific, after potentiostatic treatment under ORR conditions (**ii**) the following chronoamperometric response at 1.8 V shows higher current in the initial stage (at around 30 min-red curve) in comparison to the current response in the last stage of the **i)** treatment (Fig. S6b at around 25 min-blue curve).

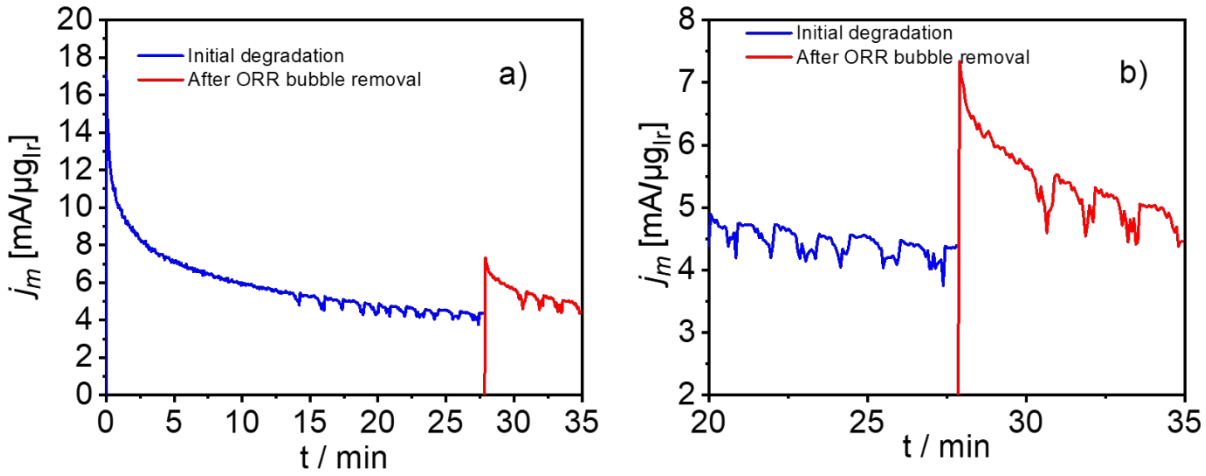

Figure S-10: Chronoamperometric curves during potentiostatic treatment at 1.8 V vs RHE. The red line is a continuation of initial potentiostatic treatment which was interrupted in order to perform a cathodic chronoamperometry at 0.3 V vs RHE during which oxygen reduction reaction took place. 4 µg of Ir catalyst was dropcasted on a BDD disc electrode resulting in a geometric loading of 20.4 µgcm$^{-2}_{geom}$.